Supplementary Material to Seja *et al.*

Supplementary Figures

Supplementary Figure S1

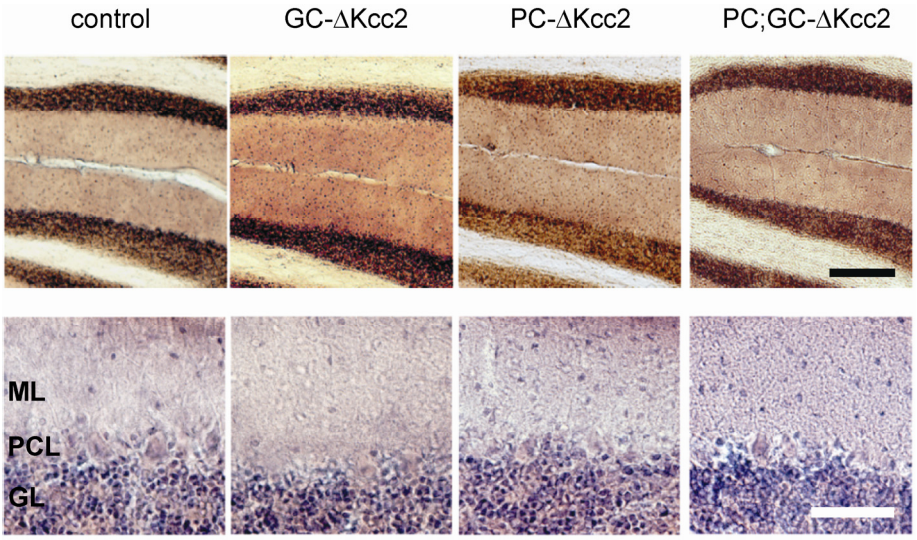

Cerebellar architecture, as well as inhibitory and excitatory synapses in the cerebellar cortex appear unchanged upon cell-specific *Kcc2* deletion. HE-staining of parasagittal cerebellar sections of 24 week-old mice. Cerebellar folia (upper panels) and cortical layers (lower panels) of control (*Kcc2*$^{lox/lox}$), Purkinje cell specific *Kcc2* KO (PC-ΔKcc2), granule cell-specific *Kcc2* KO (GC-ΔKcc2) and combined *Kcc2* KO (PC;GC-ΔKcc2) reveal normal overall morphology, normal layering of granule cell layer (GL), Purkinje cell (PC) layer and molecular layer (ML), normal layer thickness and normal cell density within layers. Scale bars: 50µm (upper panels) and 200µm (lower panels).

Supplementary Figure S2

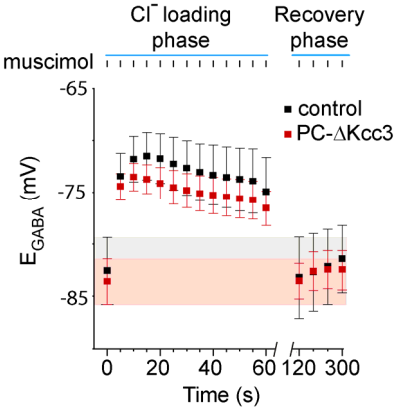

Time course of E_{GABA} during and after Cl^- loading phase for PC-ΔKcc3 mice (n=8) and control littermates (n=5). Experiments were performed as in Fig. 5E,F. Colored backgrounds display initial E_{GABA} of each genotype. Plots display averages ± SEM. Age of mice: P30-P32.

Supplementary Figure S3

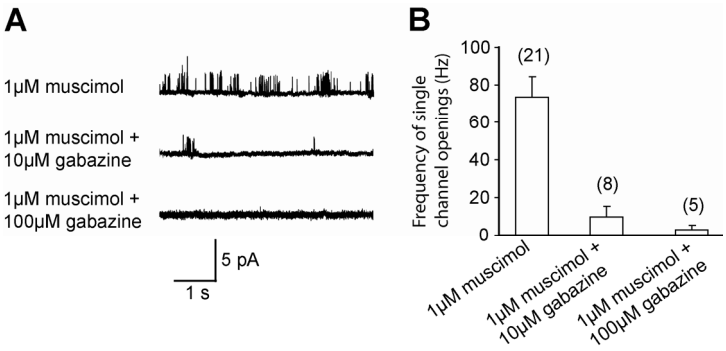

Block of $GABA_A$Rs in granule cells. (**A**) Typical single-channel recordings in cell-attached patches of GCs at a pipette potential of +80 mV. In all three traces, patch-pipettes contained 1 μM muscimol to activate $GABA_A$Rs. Single channel events were progressively blocked when 10 μM (middle trace) or 100 μM (bottom trace) of the $GABA_A$R-blocker gabazine were included. (**B**) Quantitative evaluation of experiments as in (A). The frequency of single-channel openings in the presence of muscimol is shown for different gabazine concentrations. Number of experiments is shown above each column, error bars are SEM. Age of mice: P31-P54

Supplementary Figure S4

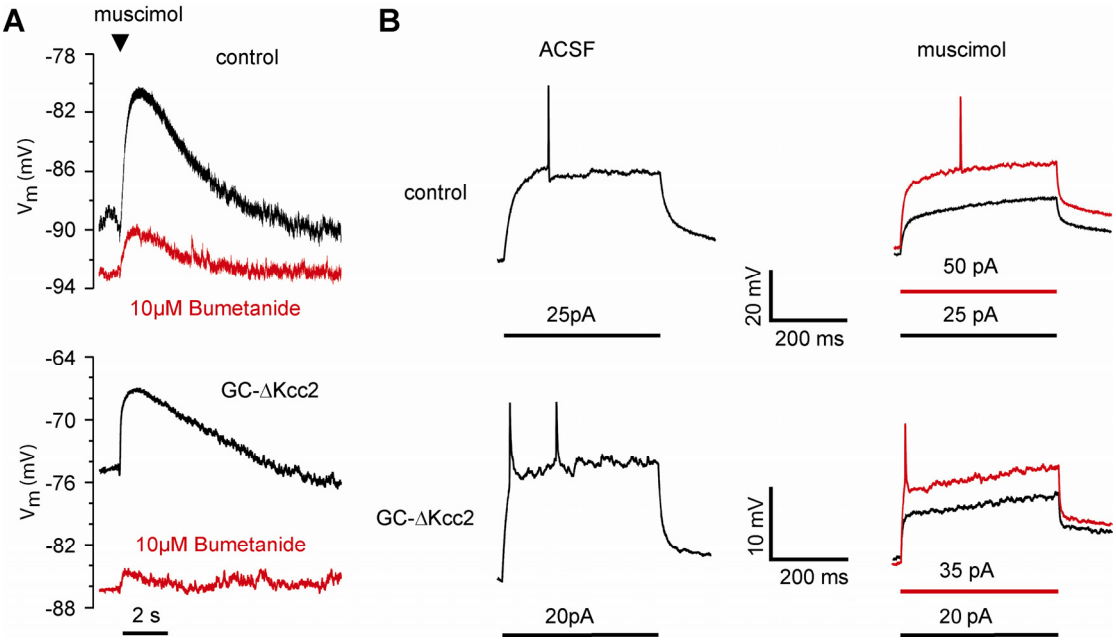

Perforated patch recordings in current clamp on GCs from control and GC-ΔKcc2 mice. (**A**) With I=0, the resting V can be read out. Application of the $GABA_A$ receptor agonist muscimol (30 ms, 50 µM) elicited a small depolarization in both genotypes (control: 6.6 ± 0.5 mV (n=14) and GC-ΔKcc2: 5.2 ± 0.6 mV (n=20)). Upon wash-in of 10µM bumetanide for 2 minutes, GCs hyperpolarized and the response to muscimol decreased. Similar results were obtained with 8 cells (3 WT, 5 KO). (**B**) Electrical excitability of GCs of either genotype in the absence or presence of muscimol. Starting from a holding current of I=0, currents of increasing amplitude (indicated below traces) were injected until action potentials were generated. Access resistance was similar for all cells (roughly 70 MΩ). To reach spike threshold we had to inject 33.6 ± 5.5 pA for control GCs, but only 16.4 ± 1.8 pA (n=7 and 9) for the depolarized GC-ΔKcc2 cells (p=0.01). The voltage threshold for spiking itself appeared unaltered (control: -54.7 ± 3.1 mV (n=7) and GC-ΔKcc2: -49.6 ± 3.0 mV (n=9), p = 0.26). (right) Upon simultaneous application of muscimol (right panels) the injected current had to be increased to elicit spiking in both genotypes because of the shunt introduced by activated $GABA_A$ receptors. Age of mice: P28 - P41.

Supplementary Figure S5

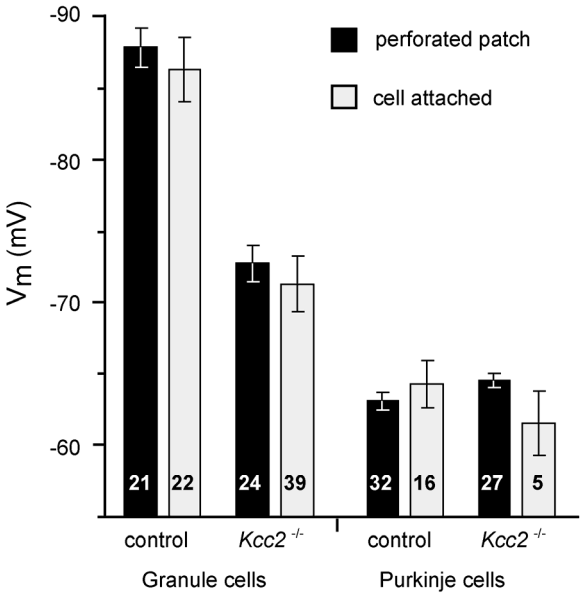

Resting membrane potentials determined by current clamp measurements in the perforated patch configuration and by cell attached measurements as described in Figure 6B reveal identical results irrespective of the method used. Error bars, SEM; numbers in bars indicate number of measurements. Age of mice: P25 - P64.

Supplementary Figure S6

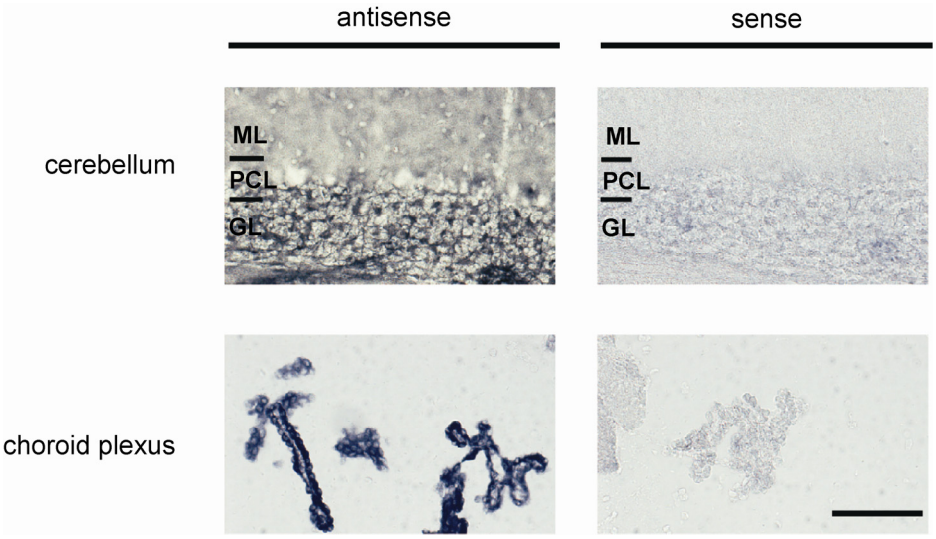

Expression of *Nkcc1* mRNA in cerebellar granule cells. *In situ* hybridization of *Nkcc1* mRNA on sagittal sections of cerebellar cortex from adult control mice (C57Bl6). The probe was directed against the sequence of exons 15-19. Hybridization of the antisense probe was observed in granule cells. Choroid plexus served as a positive control (Kanaka *et al*, 2001). Hybridization with the sense probe revealed only background staining. Scale bar: 100 µm.

Supplementary Figure S7

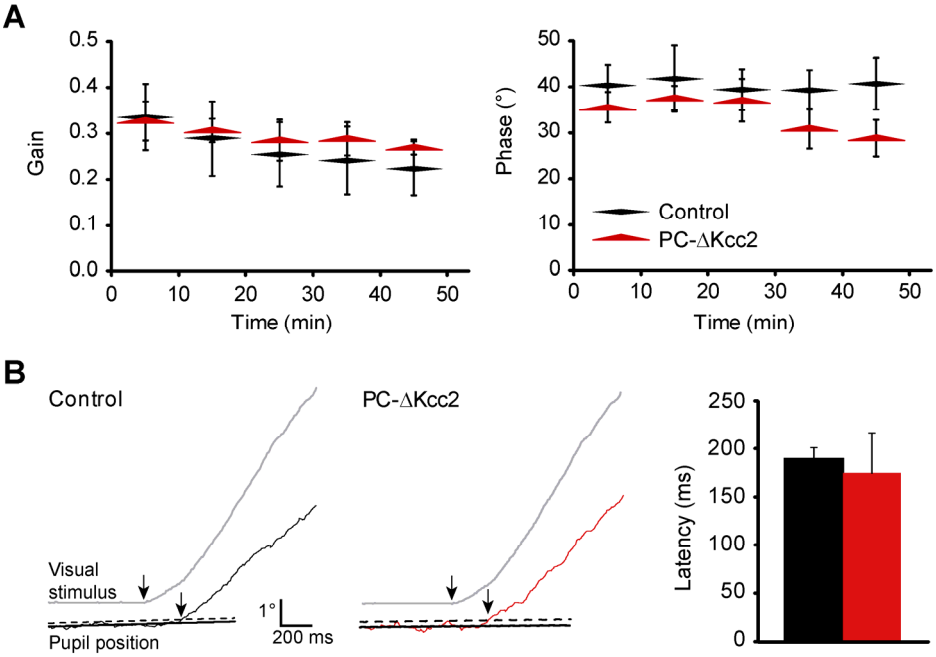

L7/pcp2::Cre driven Kcc2 deletion in the retina does not account for deficits in VOR adaptation. In the brain the L7/pcp2::Cre promoter is specific for cerebellar Purkinje cells, but is also active in retinal bipolar cells. To test whether observed deficits in VOR adaptation could be attributed to this retinal expression, we performed additional analyses of the amplitude and timing of visually driven eye movements in PC-ΔKcc2 mice. (**A**) If retinal deficits were to contribute to the deficit in VOR gain-decrease learning, one would expect to observe an inaccurate response to the training stimulus. However, the gain and phase during the training, in the light, did not differ between PC-ΔKcc2 and control mice (p=0.73 and 0.30, respectively, repeated measures ANOVA). (**B**) Theoretically, differences in response during training could be obscured by the large number of sinusoidal repeats. To quantify individual responses, we analyzed the latency of responses (red / black) to a visual stimulus (grey). The time between stimulus onset (left arrow) and pupil position crossing (right arrow) a line marking the average (thick solid) plus two SDs (thick dashed) was determined (see Suppl. Methods for details). Here too, we found no change in response latency in PC-ΔKcc2 mice compared to controls (p=0.96, Student's t-test). Together these results strongly argue against the contribution of retinal Cre expression to the observed phenotype.

Supplementary Methods

Mice

To generate *Kcc2*$^{lox/lox}$ mice, a partial genomic clone of murine *Kcc2* gene (*Slc12a5)* was isolated from a 129/Sv mouse genomic library in λFixII (Stratagene). A loxP site was inserted into intron 5, and a neomycin resistance (NEO) cassette flanked by loxP sites into intron 1. After electroporation into R1 ES cells, the NEO cassette was removed from correctly targeted clones by transfection with a plasmid expressing Cre-recombinase. Correct clones were injected into C57/Bl6 blastocysts that were implanted into foster mothers. Male chimeras carrying the *Kcc2*^{lox} allele (Fig. 1B) were bred with C57/Bl6 females to yield *Kcc2*$^{lox/+}$ mice. The generation of *Kcc3*$^{lox/+}$ mice followed essentially the procedure described above for *Kcc2*$^{lox/+}$ mice. For *Kcc3*$^{lox/lox}$ mice we started from partial genomic clones of murine *Slc12a6* from a 129/Sv mouse genomic library in λFixII (Stratagene). A loxP site and an additional SpeI site were inserted into intron 4, and a second loxP site was inserted between exons 5 and 6 (Fig. 2A).

Age of mice is indicated in figure legends, where 'adult' refers to mice older than 6 weeks.

Electrophysiology

Brains from decapitated mice (P25-21 weeks) were placed into cold "low Ca^{2+}" artificial cerebrospinal fluid (ACSF) containing the following (in mM): 119 NaCl, 2.5 KCl, 0,5 $CaCl_2$, 1.3 $MgSO_4$, 1 NaH_2PO_4, 26 $NaHCO_3$, and 11 glucose, which was gassed with 95% O_2 / 5% CO_2 (carbogen). Brains were cut in 200 µm thick sagittal slices with a vibratome (Leica). After equilibration in ACSF at RT for ≥90 min, slices were placed in a recording chamber and continuously superfused with carbogen-gassed ACSF at 22–24 °C. ACSF for perfusion contained (in mM): 119 NaCl, 2.5 KCl, 1.3 $MgSO_4$, 1 NaH_2PO_4, 26 $NaHCO_3$, 2.5 $CaCl_2$ and 11 glucose. PCs and GCs were identified with DIC video microscopy by their location and shape.

Gramicidin-perforated patch-clamp recordings were performed from PCs to determine resting membrane potential (V) and E_{GABA}. For recordings, ACSF

was supplemented with 1 µM tetrodotoxin (TTX, Sigma), 50 µM D-(-)-2-amino-5-phosphonopentanoic acid (D-AP5, Tocris), 10 µM 6-Cyano-7-nitroquinoxaline-2,3-dione (CNQX, Tocris). Pipette resistances were 2-6 MΩ. Pipette solution consisted of (in mM): 140 KCl, 5 $MgCl_2$, 10 HEPES and 5 EGTA, pH 7.3. Gramicidin (Sigma) was added to a final concentration of 5 to 50 µg/ml. Recordings with an access resistance >30 MΩ were discarded. Potentials were corrected off-line for series resistance. V was determined with a MultiClamp 700B amplifier (Molecular Devices) in current-clamp mode with I=0. GABA reversal potential (E_{GABA}) of PCs was measured in voltage clamp mode. 100 µM GABA (Sigma) or 50 µM muscimol (Sigma) was applied focally by pressure application (30 ms, 4-6 psi, Pressure System IIe, Toohey Company) from a pipette (2-4 MΩ) with the tip located close to the soma. For recordings of PCs, ACSF was supplemented with 1 µM tetrodotoxin (TTX, Sigma), 50 D-AP5 (Tocris) and 10 µM CNQX (Tocris). Cells were clamped to voltages from -140 mV to -40 mV in steps of 5-10 mV. During these steps 100 µM GABA (Sigma) or 50 µM muscimol (Sigma) was applied focally by pressure application (30 ms, 4-6 psi, Pressure System IIe, Toohey Company) from a pipette (2-4 MΩ) with the tip located close to the soma.

Gramicidin-perforated patch-clamp recordings of GCs were done in current clamp mode in the absence of TTX. Recordings started when the access resistance was <100MΩ.

Electron microscopy

Adult mice were perfused with 4% paraformaldehyde (PFA) and 2.5% glutaraldehyde (vol/vol) in phosphate buffer (0.1 M, pH 7.4). Cerebella were postfixed in the same solution overnight and processed as described previously (Andreescu *et al*, 2007). Ultrathin sections were stained with DAB-Calbindin (pre-immuno) and goldstaining (de Zeeuw *et al*, 1989) (GABA post-immuno). From tissue blocks of each mouse, 16 electron micrographs were taken randomly from the granular cell layer as well as from the molecular layer at a magnification of 19,000 to compare the morphology and density of inhibitory terminals, the density of parallel fiber to Purkinje cell synapses, and

the morphology of Purkinje cell spines. The images were stored on an HDD for later off-line analysis (MetaVue 4.6). GABA gold staining was analyzed as described previously (de Zeeuw *et al*, 1989). Results are presented as Means and Standard Error of Mean (SEM). For statistical analyses repeated measures two-way ANOVA, One-way ANOVA, Students t-test, Paired Samples Students t-test and Turkey HSD post-hoc tests were used to determine significant difference.

Eye movement recordings

All experiments involving animals were conducted in accordance with The Dutch Ethical Committee for animal experiments (DEC, Utrecht). Mice (12–30 weeks-old) were surgically prepared under general anesthesia with isoflurane/O_2. A pedestal was attached with two nuts to the frontal and parietal bones using Optibond (Kerr) and Charisma (Heraeus Kulzer). The temperature of the animal and the depth of the anesthesia were constantly monitored, and if necessary, the mice received analgesic treatment after the surgery (Temgesic / buprenophine subcutaneous injection 0.015 mg/kg). After 3 days of recovery the animals were placed in a restrainer with the pedestal fixed to a metal bar. The restrainer was fixed onto the turntable, which was surrounded by a cylindrical screen (diameter 63 cm) with a random-dotted pattern surrounding the turntable (diameter 60 cm). Eye movements (OKR and (V)VOR) were evoked by rotating the screen and/or turntable at different frequencies (Ac servo-motors, harmonic drive AG). The positions of table and drum were recorded by potentiometers and stored for off-line analysis. Eye movements were recorded, as previously described (Stahl *et al*, 2000), with the use of an infrared CCD camera fixed to the turntable (240 Hz, ISCAN Inc.). Two table-fixed infrared emitters illuminated the eye during the recording, and a third emitter was aligned horizontally with the camera's optical axis so as to produce a corneal reflection (CR). Prior to experiments the animals received one training session (1 h in the restrainer) for habituation. Mice were then subjected to baseline measurements and training sessions for 5 consecutive days. The pupil positions were computed as described (Hoebeek *et al*, 2005; Stahl *et al*, 2000; van Alphen *et al*, 2001).

Gain and phase of eye movements were calculated offline using custom-made Matlab routines (The MathWorks, Natick, MA, USA) (Goossens *et al*, 2004; van Alphen *et al*, 2001). In short, the recorded pupil position is differentiated to velocity, filtered to remove fast phases ('saccades'), and sine wave is fitted to the averaged response. Gain is defined as the ratio between the amplitude of the fitted sine and that of the stimulus, and phase as their time difference in degrees. Consolidation was calculated by dividing the minimal gain or phase change carried onwards to the next day by the maximal change achieved during the initial day (i.e. 100 * (a – c) / (a – b), see Fig. 8). Phase consolidation values of day 2 to 3, 3 to 4 and 4 to 5 (there is no phase learning on day 1) were averaged per mouse to obtain a single phase consolidation value. Latency of response the visual stimulus was determined using the initial part of 2 responses to sinusoidal OKR stimulation at 0.4Hz with 5º amplitude. The two responses were averaged after matching of the start of stimulation. Latency was calculated as the time between stimulus onset and the first crossing with the line of the average + 2 SDs (average and SD calculated for the previous 500 ms).

Supplementary References

Andreescu CE, Milojkovic BA, Haasdijk ED, Kramer P, De Jong FH, Krust A, De Zeeuw CI, De Jeu MT (2007) Estradiol improves cerebellar memory formation by activating estrogen receptor beta. *J Neurosci* **27:** 10832-10839

de Zeeuw CI, Holstege JC, Ruigrok TJ, Voogd J (1989) Ultrastructural study of the GABAergic, cerebellar, and mesodiencephalic innervation of the cat medial accessory olive: anterograde tracing combined with immunocytochemistry. *The Journal of comparative neurology* **284:** 12-35

Goossens HH, Hoebeek FE, Van Alphen AM, Van Der Steen J, Stahl JS, De Zeeuw CI, Frens MA (2004) Simple spike and complex spike activity of floccular Purkinje cells during the optokinetic reflex in mice lacking cerebellar long-term depression. *Eur J Neurosci* **19:** 687-697

Hoebeek FE, Stahl JS, van Alphen AM, Schonewille M, Luo C, Rutteman M, van den Maagdenberg AM, Molenaar PC, Goossens HH, Frens MA, De Zeeuw CI (2005) Increased noise level of Purkinje cell activities minimizes impact of their modulation during sensorimotor control. *Neuron* **45:** 953-965

Kanaka C, Ohno K, Okabe A, Kuriyama K, Itoh T, Fukuda A, Sato K (2001) The differential expression patterns of messenger RNAs encoding K-Cl cotransporters (KCC1,2) and Na-K-2Cl cotransporter (NKCC1) in the rat nervous system. *Neuroscience* **104:** 933-946

Stahl JS, van Alphen AM, De Zeeuw CI (2000) A comparison of video and magnetic search coil recordings of mouse eye movements. *J Neurosci Methods* **99:** 101-110

van Alphen AM, Stahl JS, De Zeeuw CI (2001) The dynamic characteristics of the mouse horizontal vestibulo-ocular and optokinetic response. *Brain Res* **890:** 296-305